Swansea University
Prifysgol Abertawe

Cronfa
Setting Research Free

# Cronfa - Swansea University Open Access Repository

_____

This is an author produced version of a paper published in:
*The Journal of Physical Chemistry C*

_____

Cronfa URL for this paper:
http://cronfa.swan.ac.uk/Record/cronfa52512

_____

_____

http://www.swansea.ac.uk/library/researchsupport/ris-support/

# The Diffusion of Au(CH₃S)₂ on Au(111) Observed with the Scanning Tunneling Microscope

Scott Holmes,[§] Richard E Palmer,[$] and Quanmin Guo[§*]

[§] *School of Physics and Astronomy, University of Birmingham*
*Edgbaston, Birmingham, B15 2TT, UK*
[$]*College of Engineering, Swansea University, Bay Campus, Fabian Way, Swansea, SA1 8EN, UK*

**ABSTRACT:** The diffusion of a three-legged molecule, $CH_3S$-Au-$SCH_3$, on Au(111) has been investigated using scanning tunnelling microscopy. Each of the two S atoms forms a bond with a Au atom in the Au(111) substrate. The Au atom in the molecule provides the third anchoring point via its interaction with Au(111). $CH_3S$-Au-$SCH_3$ hops as a single unit without breaking any of the S-Au bonds within the molecule at temperatures below 170 K, with an activation energy of 66 meV. The $CH_3S$-Au-$SCH_3$ molecules have a tendency to aggregate into rows driven by an attractive potential between neighbouring molecules, with the minimum row consisting of just two molecules in the form of a dimer. The dimer is much less mobile than a single molecule due to the attractive potential between the two molecules. The dimer is observed apparently to hop as a single unit with an activation energy of 210 meV. Detachment of a $CH_3S$-Au-$SCH_3$ molecule from the end of a row consisting three or more molecules takes place with an activation energy of 320 meV.

---

[*] Email: Q.Guo@bham.ac.uk

## 1. Introduction

Self-assembled monolayers (SAMs) of alkanethiols on gold surfaces have been studied extensively[1-6] for both the fundamental interest in molecular self-assembly and the potential applications of thiol-passivated Au nano-particles[7-12]. The alkanethiol SAM consists of a basic building block, RS-Au-SR, which is commonly known as the staple motif[12]. The staple has three contact points to the gold substrate[3, 12]: two through the bonding between the S atoms and gold atoms within the first layer of Au(111); one from the bonding between the Au atom of the staple and substrate Au atoms. The staple is rather mobile if the alkane chain is short[13-15]. For example, the $CH_3S$-Au-$SCH_3$ staple molecule is found in a two-dimensional gas phase at room temperature (RT)[13]. Because of the multi-point contact between the molecule and the substrate, the surface diffusion of such a molecule becomes an interesting issue. The diffusion of $CH_3S$-Au-$SCH_3$ has previously been studied using DFT calculations[16] which give rise to an activation barrier of the order of ~0.5 eV. As far as we know, the diffusional behavior of this molecule has not been quantitatively studied experimentally. For RS-Au-SR with a long alkane chain, the van der Waals interaction between neighboring RS-Au-SR is strong enough to inhibit surface diffusion. For $CH_3S$-Au-$SCH_3$, the contribution of the van der Waals interaction is minimized. Therefore, the diffusive behavior is affected mainly by the bonding between the staple and the Au(111) substrate. For simplicity, we will refer $CH_3S$-Au-$SCH_3$ as $Au(CH_3S)_2$, although AAD (Au-adatom-dithiolate) has also been used in literature[17].

In this paper, we report findings from a scanning tunneling microscopy (STM) study of the diffusive characteristics of $Au(CH_3S)_2$ in the temperature range between 77 K and 190 K. We measured the hopping frequency of individual $Au(CH_3S)_2$ at different temperatures and extracted an activation energy for diffusion by fitting the data to an Arrhenius type of expression. $Au(CH_3S)_2$ molecules have a tendency to form rows along the $[11\bar{2}]$ direction for a broad range of coverages due to an attractive interaction between nearest neighbor molecules[6,13]. This row structure is rather common and observed for alkyl-thiolates with different alkane lengths[18, 19]. An $Au(CH_3S)_2$ molecule can break off from the end of a $Au(CH_3S)_2$ row in a thermally activated process. Measuring the frequency of the break-off event at different sample temperatures allows us to obtain an activation energy for this process. Below 170 K, $Au(CH_3S)_2$ always moves as a single unit. At higher temperatures, the molecule is expected to be able to dissociate allowing for ligand exchange between different $Au(CH_3S)_2$ staples,

as observed for $Au(CH_3CH_2-S)_2$ at room temperature [20]. The high density, (3x4), phase of $Au(CH_3S)_2$ is not studied here because diffusion within such a phase requires the presence of molecular vacancies which are extremely rare for the (3x4) phase[13]. Our findings help to understand the detailed mechanism of $Au(CH_3S)_2$ diffusion on Au(111) and how the interaction between individual $Au(CH_3S)_2$ molecules and $Au(CH_3S)_2$ rows affects the assembly of the striped phase of the $Au(CH_3S)_2$ SAM.

## 2. Methods

A (111)-oriented Au single crystal is used for the experiment. The sample is cleaned by standard $Ar^+$ ion sputtering and thermal annealing cycles. The clean Au(111) is then exposed to dimethyldisulfide (DMDS) at room temperature to reach full surface coverage. This is followed by thermal annealing at 350 K to desorb some molecules. After cooling to 77 K, the sample is imaged with an Omicron low temperature STM (LT-STM) with an electrochemically etched tungsten tip, and shows the typical striped phase[13].

At room temperature, the molecules are not stably arranged on the surface, and instead form a kind of 2D gas phase[21] except for the highest coverage phase in which the molecules are locked in position by neighboring molecules. Upon cooling to 77 K to perform the experiments, this gas of molecules on the surface condenses to form the $Au(CH_3S)_2$ rows. This process is achieved very rapidly on contact of the sample with the cryostat, held at 77 K. By studying the system at a variety of temperatures, it is possible to determine the processes that can take place during this rapid cool down, and how they could potentially affect the final system arrived at. A rapid cool down essentially freezes the $Au(CH_3S)_2$ rows after a short formation time, resulting in only the short rows that form before the diffusion rate drops significantly. The formation of long-range ordered structures is kinetically hindered.

In order to study these processes in detail a series of images were taken of several surface areas for every 10 K increments between 90 K and 190 K. The series of images was then aligned to a high precision using an algorithm, allowing for comparisons of sequential pairs of images in the series and highlighting any changes, which were then labeled. An attempt was made to identify the initial and final positions of all $Au(CH_3S)_2$ that were involved in a thermally triggered event. To avoid the STM tip having an influence on the thermal processes imaging was conducted at low currents and reasonably high bias. The parameters used were 500 mV sample bias

and 50 pA tunnel current. These parameters do not permit very high-resolution images, but the image quality is sufficient to identify motion of the $Au(CH_3S)_2$.

If the probability of a process happening is very large, then it will happen many times during a single STM image. This typically appears as streaking or blurring of features in the STM image, as the species being imaged moves under the tip between scan lines, or even within them. On the other hand, if the probability of a process occurring is very small, then the process will only occur very rarely and may not be seen by the experimenter during the timeframe of the experiment. In between these extremes the number of events which happen during an image can be counted. This leads to a histogram of events against time, where the bin size is given by the length of time taken to record the STM image (5 minutes). In order to normalize the probability it is necessary to have an estimate of the number of molecules that could undergo each process in an image; for instance single $Au(CH_3S)_2$ diffusion needs a count of single $Au(CH_3S)_2$ which could diffuse in order to determine how probable diffusion is. To determine the $Au(CH_3S)_2$ row populations, all of the rows on the initial image of the series were labeled by their endpoints to provide an estimate of the initial population of rows and their length distribution. This population was then adjusted by taking into account the measured alterations in row lengths over the series to give a population for each image in the series. The time between images is used, together with the initial populations, to generate a probability per unit time of a single $Au(CH_3S)_2$ undergoing some process.

## 3. Results and discussion

At temperatures below 130 K the diffusive behavior is uncomplicated. Most $Au(CH_3S)_2$ are stable and do not move. Figure 1a shows an STM image acquired at 100 K. At the top of the image, there is a short, horizontally oriented, $Au(CH_3S)_2$ row consisting of five $Au(CH_3S)_2$ molecules. The formation of such rows aligned in the [11$\bar{2}$] direction is a well known phenomenon[3, 6]. Close to the center of the image, there is one single $Au(CH_3S)_2$ not attached to other molecules. This kind of isolated $Au(CH_3S)_2$ molecules are capable of diffusion over the surface, usually to the nearest unoccupied bonding location on the gold lattice. Figure 1b shows an STM image from the same area after the isolated $Au(CH_3S)_2$ has displaced sideways to the nearest-neighbor bonding site. High-resolution images and structural models illustrating the bonding configuration of $Au(CH_3S)_2$ can be found in Ref. [13]. Fig. 1c gives a schematic model showing how $Au(CH_3S)_2$ is bonded to Au(111). The centre of mass of

Au(CH$_3$S)$_2$ is located at the Au adatom which is bridge-bonded to Au atoms in the underlying Au(111). The red dots in the images represent the bridge sites of the Au(111) surface. The gold lattice vectors are deduced by using the lattice vectors of the Au(CH$_3$S)$_2$ rows, together with the structural model of the Au(CH$_3$S)$_2$ bonding location[13]. Using this derived lattice, it is possible to determine where a Au(CH$_3$S)$_2$ diffuses to relative to its initial position. This also allows the number of diffusive hops to be evaluated. If multiple hops occur during the time taken to record an image, only the final location will be seen. Under the present experimental conditions, diffusion events are rare as most molecules do not move at all during two successive scanning frames. The ones that do move are observed to take a single hop over the duration of many scanning frames. Therefore, when a molecule is found to have displaced in between two successive frames, it can be assumed that the displacement is completed with one single hop. This assumption is not valid for high temperatures when single molecules diffuse much more frequently. We found that individual Au(CH$_3$S)$_2$ molecules displace from one site to the nearest neighbor site in a single hop as illustrated in Fig. 1d where the yellow stick represents the proposed transition state. The position of a molecule in Fig. 1a is marked by a green dot before the displacement. The blue dot indicates the destination of the molecule after the hop. As shown in Fig. 1d), the molecule hops along one of the close-packed atomic directions on Au(111) in steps of $a$ where $a$ is the nearest neighbor distance for Au atoms. In the proposed transition state shown in Fig. 1d), the Au adatom occupies the bridge site as usual, the S atoms have shifted from their preferred atop site to bridge site. Although it appears possible for the molecule to hop onto other sites via a combination of translational and rotational movements, we do not observe molecules moving further than the nearest neighbor bonding site in a single hop at this temperature. At 100 K, the only movement observed is from isolated Au(CH$_3$S)$_2$ molecules. The molecular rows are stable showing no change within many hours of scanning. Detachment of a molecule from either end of the molecular row is readily observed when the temperature of the sample is increased, as will be described later. Due to the three-fold symmetry of the substrate, the molecular axis of Au(CH$_3$S)$_2$ can take any three equivalent directions as indeed observed in our experiment. When a Au(CH$_3$S)$_2$ takes a single hop, it seems to keep the orientation of its molecular axis un-changed in a simple translation. This phenomenon will be further discussed later with Figure 3(d).

To normalize the diffusion probability, the number of single molecules available to diffuse has been counted. This can be used, together with the time taken between images, to provide a diffusion probability per unit time. Several

series of images were taken, and for each image the total number of diffusive hops (calculated as described in the previous paragraph) was normalized against the population of single $Au(CH_3S)_2$ over the image, before dividing by the total imaged time to give a probability per unit time. This is shown plotted on a semi-log plot against $1/T$ over the full range of temperatures in figure 2. The value plotted for a temperature is the mean of all of the values measured from the images at that temperature. The errors are the standard error on that mean. The two points in a lighter blue color on the upper left were not taken into account for the exponential fit as diffusion rates are difficult to quantify at these "high" temperatures. The simple model that the molecule hops one single step in between two scanning frames breaks down at high temperatures. A more complicated model involving random walks would need to be developed.
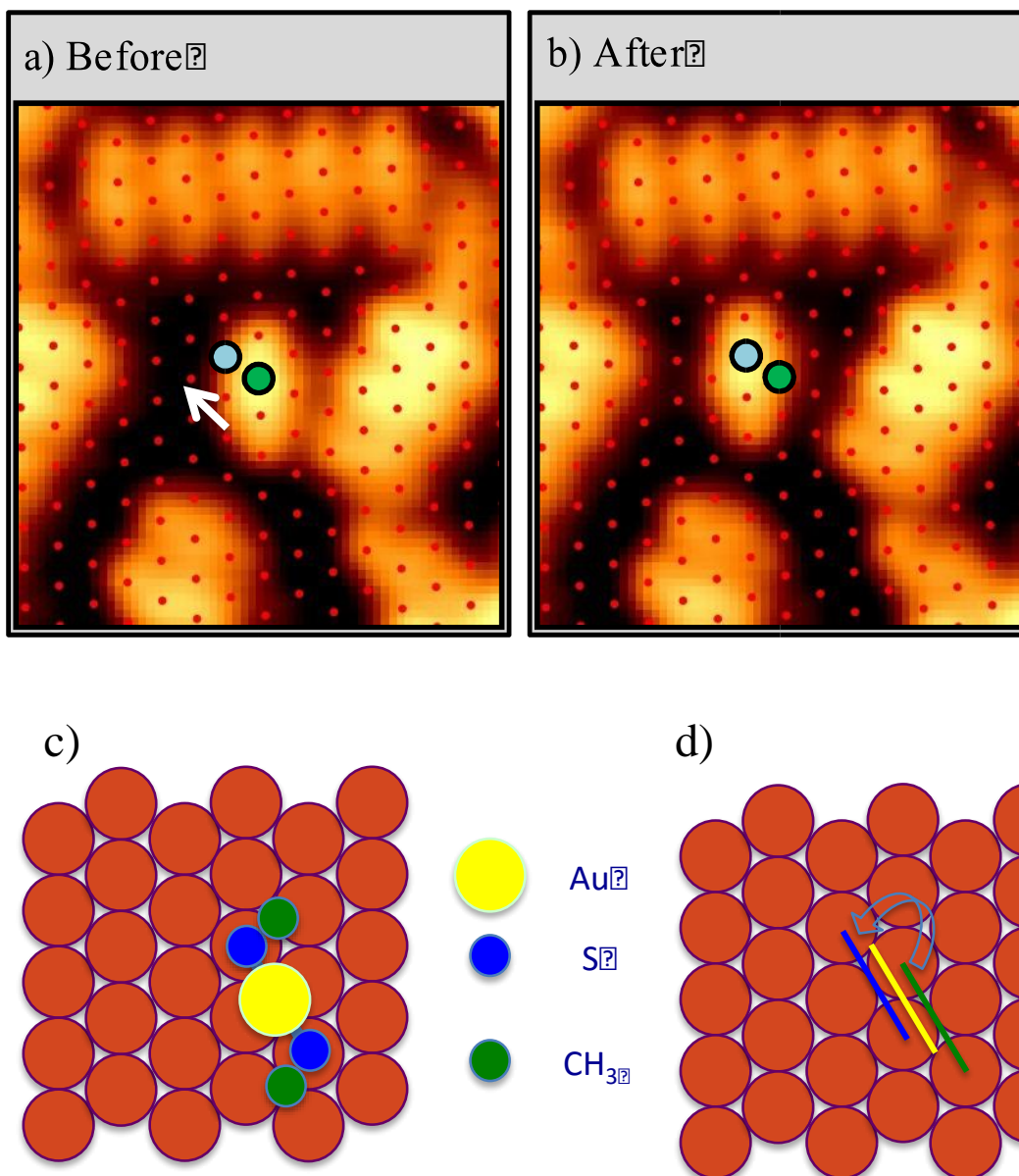
**Figure 1.** Panels a) and b) show a single $Au(CH_3S)_2$ molecule in two consecutive STM images at 100 K. The initial and final Au-adatom locations are marked in green and blue, respectively. The red dots in both images mark the locations of bridge sites in the underlying Au lattice, deduced from the positions of the $Au(CH_3S)_2$ molecules. Panel c) shows a ball model for a single $Au(CH_3S)_2$ molecule on Au(111). Panel d) illustrates how a single molecule hops between two nearest neighbor adsorption site via a transition state. The green stick represents the molecule in its initial location and the blue stick represents the molecule in its final location. In the transition state represented by the yellow stick, the Au adatom occupies the bridge site with the S atoms "bridge-bonded" to Au atoms in the substrate. The S atom sits above a bridge site, although it is not clear either this represents a true bridge bond between a S atom and two Au atoms in the substrate.
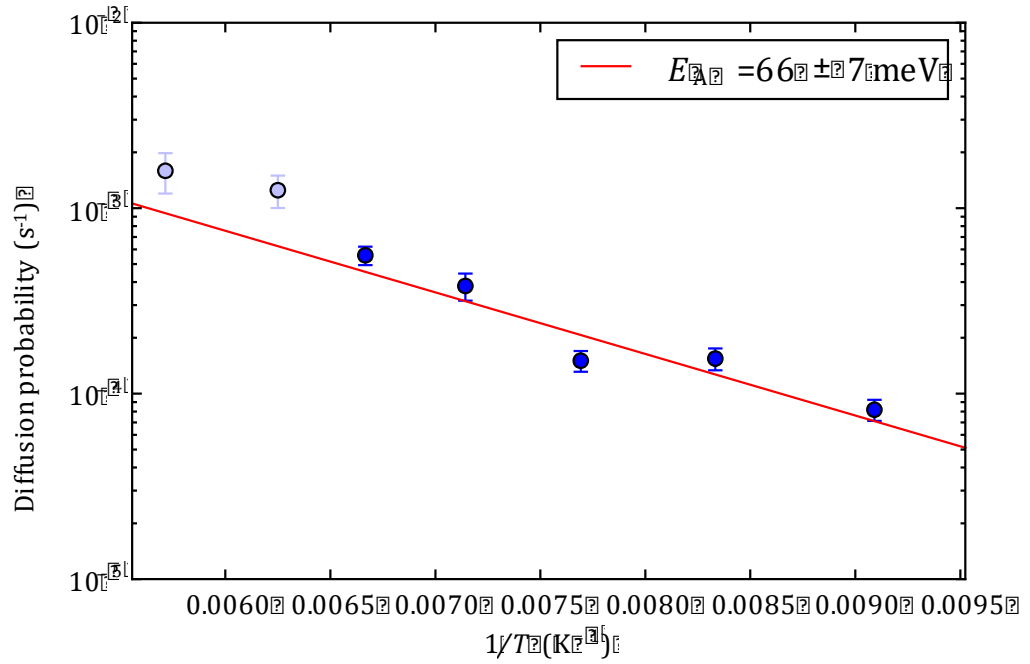
**Figure 2.** Graph showing the diffusion probability for single $Au(CH_3S)_2$ molecules per unit time plotted for a range of temperatures. Each point is the average of the measured values over $\sim 10$ images. Errors are the standard error on that mean. The two points in lighter blue on the left are excluded from the fit, as rapid diffusion of single molecules makes the diffusion difficult to quantify accurately. The red line is an exponential fit, giving the activation energy shown.

The activation barrier for the diffusive process of an isolated molecule is found to be $(66 \pm 7)$ meV. This barrier is much lower than that calculated in[16] of 0.5 eV. The low activation energy from our measurement could indicate some tip-assisted diffusion. However, our observation does not suggest a significant role played by the STM tip. When molecules move under the influence of the STM tip, characteristic signs usually appear in the image. One such sign is that a molecule disappears/appears suddenly when the tip moves close to it resulting in a fraction of the molecule being imaged by the STM[21]. In the present study, we do not observe incomplete molecules. Whenever an isolated $Au(CH_3S)_2$ appears in the image, it shows as a stable whole molecule with no signs (streaks/fuzziness) of tip-assisted motion. This indicates that the molecular hopping takes place when the tip is far away and the molecule is always imaged in its stable adsorption site. The low activation barrier could be due to the flexibility of the Au(111) surface. The clean Au(111) surface has a structure different from the bulk truncated form by having the so-called herringbone reconstruction. The herringbone reconstruction of Au(111) is lifted in the presence of $Au(CH_3S)_2$ at moderate coverages[13]. Hence, in the presence of sufficient $Au(CH_3S)_2$ molecules, the Au(111) surface could be treated approximately as a standard (111) plane of a close-packed atomic layer. The critical coverage of $Au(CH_3S)_2$ needed to lift the reconstruction is not known. However, existing experimental data[13] show that 0.1 monolayer (ML) of $Au(CH_3S)_2$ is sufficient to lift the reconstruction. The saturation coverage

is 1/3 ML corresponding to one molecule per six surface Au atoms. We do not call it 1/6 ML in order to keep consistency with notation used widely in previous publications. With the herringbone reconstruction lifted, it is usually assumed that the top layer of Au atoms uniformly resume their bulk-truncated positions as treated in calculations. This assumption, however, may not be accurate enough. In between the herringbone reconstructed surface and the bulk-truncated surface, there is the possibility that the Au(111) surface could exist in a meta-stable state in response to the nature of an adsorbate and its coverage. Such a meta-stable surface could be strained with the level of strain varies from place to place according to the local adsorbate coverage. We have no direct experimental evidence supporting the notion of a Au(111) surface in between a herringbone reconstructed state and the fully relaxed state. However, localized lifting of the reconstruction has been observed for Au(111) with a very low coverage of $Au(CH_3CH_2S)_2$ [22], where the $Au(CH_3CH_2S)_2$ rows are able to push aside the discommensuration lines. The large difference between the experimentally measured activation energy and that from calculation deserves some more thorough investigation of this system.

An interesting point to note is that the thermal energy required to break one of the S-Au bonds of $Au(CH_3S)_2$ is evidently much higher than the diffusion barrier on the surface, as $Au(CH_3S)_2$ diffuses as a whole in the temperature range studied. The barrier height to break one of the S-Au bonds in $CH_3S$-Au-$SCH_3$ was calculated to be ~ 0.6 eV[23]. Whilst hopping of individual $Au(CH_3S)_2$ is readily observed at 100 K, no sign of breaking the S-Au bond of $Au(CH_3S)_2$ is found at even 190 K. One could argue that the STM only images the initial and final states of the molecule, and hence any possible intermediate steps involving the breaking and re-making of the S-Au bond could not be recorded if these steps occur very rapidly. In order to seek further experimental evidence, we broke the S-Au bond for a number of molecules by injecting electrons to the molecules. This created -Au-$SCH_3$ and $SCH_3$ fragments. We find that these fragments are rather stable within 100 K-170 K and they do not recombine over a long time. Therefore, we can exclude the possibility of any thermally induced fragmentation of $Au(CH_3S)_2$ in this temperature range. The $Au(CH_3S)_2$ molecule is usually considered to be bonded to the surface in three locations, with the two S atoms and the Au atom all involved in bonding to the Au(111) substrate. This gives rise to a three-legged bonding configuration. It is expected that the bonding between the S atom and the Au(111) substrate has different strength from the bonding between the Au adatom and the substrate. The activation energy represents the energy required to break the stronger of the two different bonds. It was also

noticed that once a $Au(CH_3S)_2$ molecule had diffused it would often diffuse again, usually back to the starting position. It is not clear to us why the molecule prefers to move back to where it came from if the surface potential is the same for the same type of adsorption site. Maybe the presence of $Au(CH_3S)_2$ rows in the neighborhood plays some role here.

In addition to the diffusion of individual $Au(CH_3S)_2$ on Au(111), we have also observed the diffusion of short $Au(CH_3S)_2$ rows. Figure 3 demonstrates the "collective" diffusion of the shortest row which consists of just two molecules. In this case, the two molecules can diffuse to their nearest neighbor locations. It is known that there is an attractive interaction between $Au(CH_3S)_2$ molecules along the row[13]. Thus, if one of the molecules breaks away from the row, there is a tendency for the other to follow. Or, if one breaks away, it has a tendency to go back toward the other. The frequent occurrence of collective diffusion of an $Au(CH_3S)_2$ pair suggests that the diffusion takes place mostly by molecules jumping to the nearest neighbor bonding sites. This is rather similar to the hopping of single molecules described above. Fig. 3c) is a stick and ball model showing how two molecules move from their initial locations to their final locations in a seemingly concerted motion. In Fig. 3d), a number of possible destinations are highlighted for the molecule. However, the molecule does not move into these locations. The hopping process shown in Fig. 1d) and Fig. 3c) is most preferred. The diffusion probability for a row of two molecules is plotted in Figure 4, yielding an activation energy of $(210 \pm 20)$ meV. This measured activation energy is much higher than the energy required for single molecule diffusion. Most of this energy is due to the need to overcome the attractive interaction between the two molecules. The STM images of Fig. 3 indicate that the two molecules move together to new locations while maintaining a bonded pair. However, this "collective" motion is also possible the result of two individual steps with one molecule breaking away and the other follows. This becomes clearer when observing how a single molecule breaks away from a longer row.
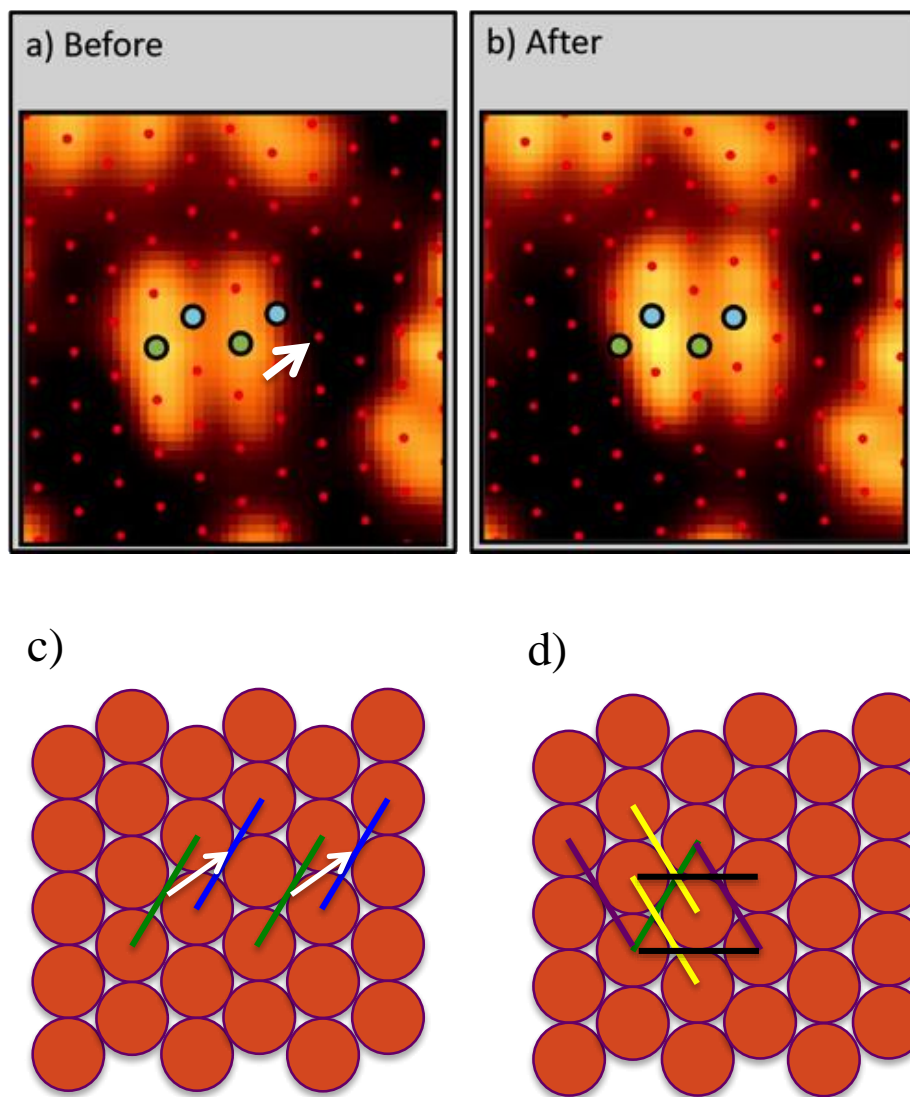
**Figure 3.** Panels a) and b) show an Au(CH$_3$S)$_2$ dimer in two consecutive STM images. The initial and final Au-adatom locations are marked in green and blue, respectively. Panel c) shows a ball model for the process, where the molecule is represented by a stick for simplicity. The white arrows illustrate the "paths" the molecules take from their initial positions (green stick) to the final positions (blue stick). d) The green stick shows the initial position of the molecule. Sticks of other colors highlight other possible destinations that the molecule does not move into.
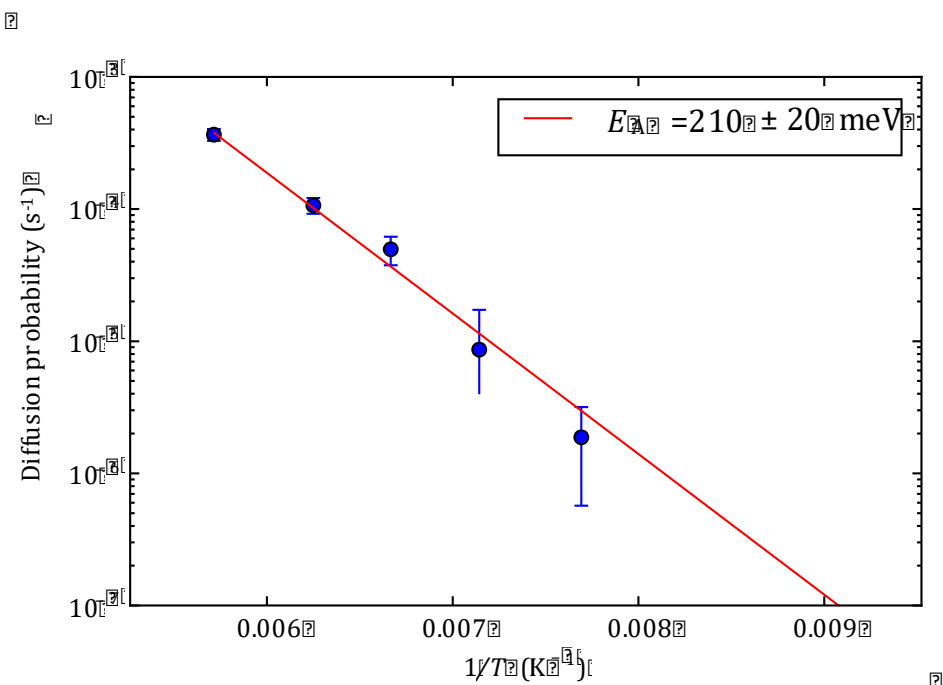
**Figure 4.** Graph showing the diffusion probability for a Au(CH$_3$S)$_2$ dimer per unit time, plotted for a range of temperatures. Each point is the average of the measured values over ~ 10 images, errors are the standard error on that mean. The red line is an exponential fit, giving the activation energy shown.

At the highest temperatures (~190 K) studied, a long Au(CH$_3$S)$_2$ row can split into shorter segments. In order for a row to break, at least one of the remnants of the row must diffuse away. The energy requirement for row breakage is dominated by the energy required to break the row, after which diffusion of a single Au(CH$_3$S)$_2$ over the surface is facile at the temperatures involved. There are several interesting quantities that can be studied for this process.

Firstly, row breakage begins to be measurable at around 140 K. At this temperature rows of two molecules long can diffuse, and single molecules can diffuse over a few nearest neighbor sites in between two frames. For 140 K $\leq T \leq$ 160 K row breakage is dominated by events where one molecule breaks off from the end of a row (making up all of the measured events). Figure 5 shows an event where a molecule becomes detached from one end of a row. The breakaway molecule in this case moves a substantial distance away from its initial position and its final position is not restricted to what is depicted in Fig. 1d). It is not clear if this molecule travels this distance in a single jump or via multiple jumps. At T>175 K, the row breaks in more complicated ways, and it becomes

12

impossible to tell whether a row immediately breaks into the fragments seen, or whether a small section breaks off before being joined by further elements.

For a single molecule to break off from the end of a row, it needs to overcome the attractive potential between two adjacent molecules in the row. Normalizing the number of single unit breaks to the number of row ends (twice the number of rows), gives the probability of a single molecule breaking off the end of a row. This is a worse normalization than for single molecule diffusion as quite often chains can end at other chains and the close packing at these junctions may hamper the breaking process, implying that the normalization overestimates the number of molecules which could diffuse, thus leading to an underestimate of the absolute probability of diffusion. However, this shouldn't affect the variation of the rate with temperature, unless the number of chains ending at other chains changes significantly. Plotting this value against temperature and fitting an exponential allows an energy barrier to be extracted.
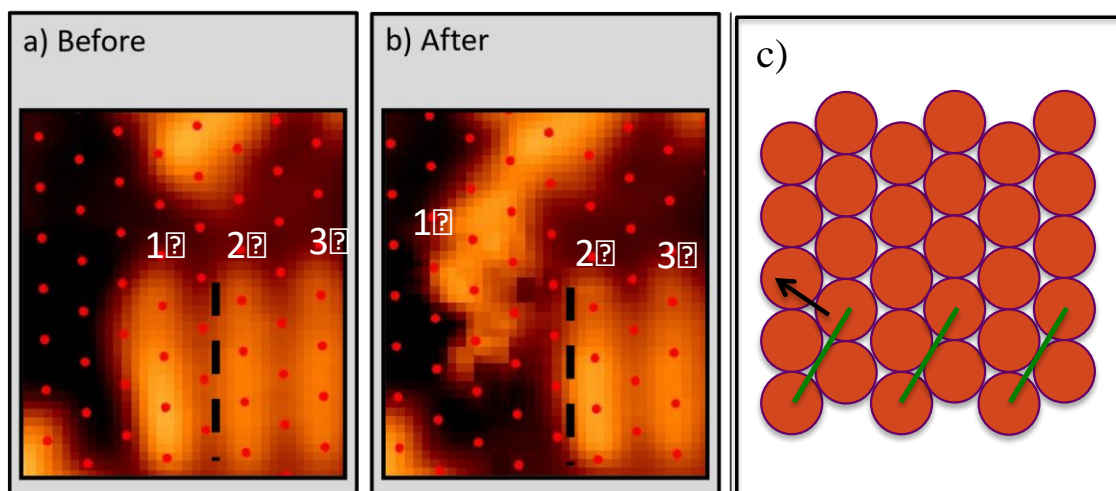


**Figure 5.**  Panel a) and b) show that a molecule at the left end (1) of a three-molecule row breaking off between two consecutive STM images. Panel c) shows a ball model of this process.
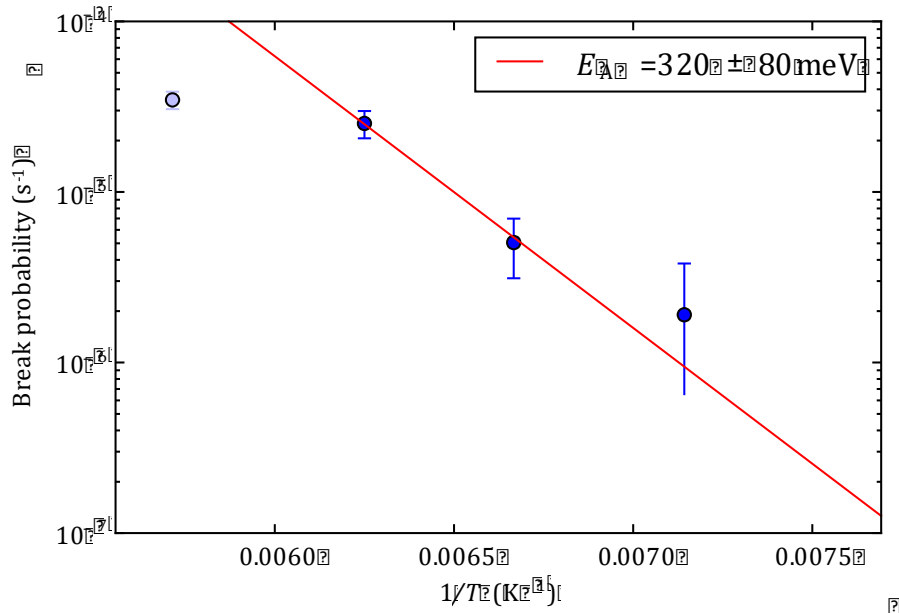
**Figure 6.** Graph showing the probability for a single molecule to break from a row per unit time, plotted for a range of temperatures. Each point is the average of the measured values over ~ 10 images, errors are the standard error on that mean. Lighter points are excluded from the fit for reasons given in the text. The red line is an exponential fit, giving the activation energy shown.

Figure 6 shows the probability of chain breakage plotted as a function of $1/T$. The leftmost point corresponds to 175 K and is ignored as a substantial number of row breaks involve many small rows, so it is not possible to unambiguously determine what happened in the break up. At the three temperatures fitted, the only breakage process occurring is the breakoff of a single unit from the one end of the row. Thus, it is possible to easily distinguish the events and normalize them. The extracted activation energy is $(320 \pm 80)$ meV, which is significantly higher than the 210 meV required for the diffusion of a dimer. The activation energy for a molecule to become detached from the end of a row is mostly contributed by the attractive potential between adjacent molecules in the row, as the energy required for a detached molecule to diffuse is only 66 meV. Therefore, the 320 meV energy can be assigned to the intermolecular bonding between a pair of molecules. For a dimer, if the collective diffusion of two molecules begins with the momentarily separation of the two, one would expect a similar activation energy of ~320 meV. Therefore, for the shortest row with only two molecules, it is possible that when one of the molecules begins to move away, the other immediately follows, giving rise to a correlated motion and reduced energy barrier. In other words, the two molecules are not completely separated during motion.

14

At the temperatures where breakage of rows becomes common, coalescence also becomes more probable as a result of the higher frequency of diffusion. The net changes in row length are then interesting, as they determine whether rows tend to grow or shrink at these temperatures. This can be determined by comparing each row-length altering event and looking at whether the average row length after the event is longer or shorter than before the event. It was found that in general rows get longer rather than shorter. This was also found to be noticeable when examining samples that had been held at elevated temperatures for extended periods. The extended gentle annealing favors long rows, and this is evident to the eye when looking at images taken after such a period. Our observation is consistent with the scheme where rows are broken mainly from the ends. Thus, as the average row length increases, the effective row breaking probability per molecule decreases because the proportion of molecules at the end of the row diminishes.

At the highest temperature studied (190 K), the rows form an interesting ordered liquid phase. $Au(CH_3S)_2$ molecules still exist and form rows, but the rows are constantly changing length and orientation, Figure 7. There is a complex interplay of attractive and repulsive interactions in this situation. Attractive interactions exist between molecules in the rows, but between rows there seems to be a repulsive interaction, evident from the tendency of the rows to space out. Rows can create interesting diffusive environments, where single molecules can diffuse onto and off of row ends, but molecules in the middle of a row cannot move easily due to the packing of the rows. Eventually (200 K+), no rows exist and the surface consists of a 2D gas. At this stage, no feature can be resolved in the STM image which only shows streaks due to fast diffusing molecules. The 2D gas phase is likely composed of $CH_3S$- and $CH_3S$-Au groups and gold atoms diffusing freely over the surface. It may of interest to examine this transition in greater detail, as it may be that the transition to the 2D gas phase occurs when the $Au(CH_3S)_2$ molecules themselves begin to break up. There is clear evidence that the RS-Au-SR staple breaks into RS and Au-SR at RT from surface reactions involving thiols of different alkane chain lengths[14,15].
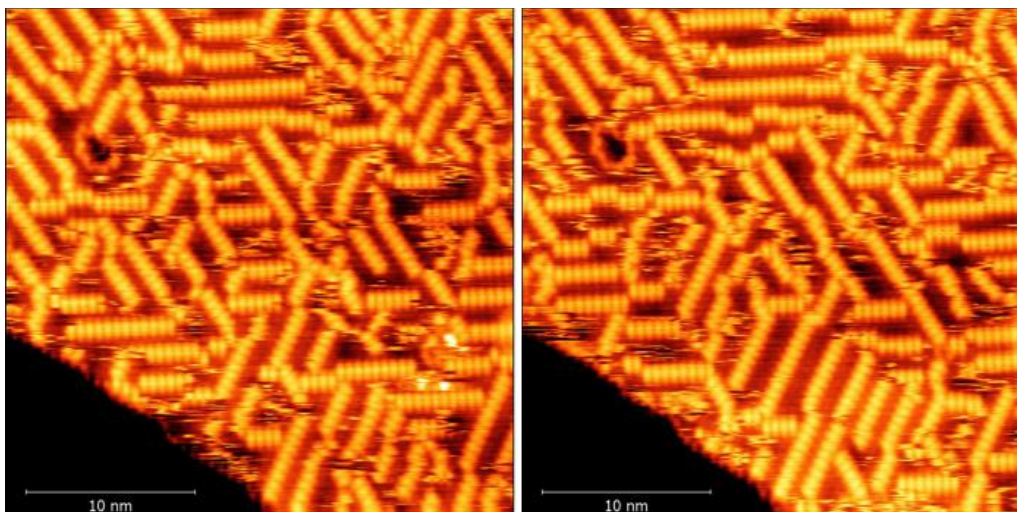
**Figure 7.** Images from the same area showing the row phase at 190 K. The rows rapidly change orientations in the time between the two consecutive images (about 5 minutes). The hazy areas between rows are rapidly diffusing molecules. Images are acquired using 0.5 V sample bias and 100 pA tunnel current.

## Conclusions

In summary, a number of interesting dynamical processes have been studied in the low coverage row phase of $CH_3S$-Au-$SCH_3$ on Au(111). These include diffusion, and row breaking. All of the dynamical processes studied were found to be thermally activated between 77 K and 190 K, and would all be facile at room temperature. The activation barrier for the diffusion of isolated $Au(CH_3S)_2$ molecules on Au(111) is determined experimentally to be $(66 \pm 7)$ meV. The activation energy for a molecule to break off the end of an $Au(CH_3S)_2$ row is determined to be $320 \pm 80$ meV. This gives a quantitative measure of the interaction strength between molecules in the row. There is some evidence of concerted diffusion of $Au(CH_3S)_2$ dimers. The correlated diffusion of $Au(CH_3S)_2$ dimers is interesting and is expected to represent the general behavior of molecular diffusion where an attractive force exists between neighboring molecules.

Within the temperature range studied, 77 K – 190 K, diffusion was found to occur mainly by the displacement of $Au(CH_3S)_2$ with no fragmentation of the molecule. With higher temperatures, breaking the S-Au bond of the molecule becomes possible and there expected to be multiple species on the surface including $CH_3S$ and $CH_3SAu$. Breaking of the S-Au bond makes ligand exchange possible[14, 20].

Long $Au(CH_3S)_2$ rows are stabilized by attractive forces within the row. The outcome of this is that rows tend to grow in length when held at intermediate temperatures, where the rows do not break up rapidly, but single molecule diffusion is relatively rapid. Single molecule can diffuse onto and off the ends of rows, but there is an energy barrier to leaving the row that is not present for attachment to the end of the row. Overall, this favors row growth.

For alkanethiols in general, the diffusion and stability of $Au(RS)_2$ is expected to be dependent on the length of R. The van der Waals interaction between the alkane chains contributes a stabilizing factor which makes it harder to thermally fragment $Au(RS)_2$ for long Rs. Detachment of a single $Au(RS)_2$ from the end of an $Au(RS)_2$ row also becomes more difficult. The length of the alkane chain also affects the bonding between $Au(RS)_2$ and the $Au(111)$ substrate. The longer alkyl chain has a higher ability to donate electrons to the S atom and hence weaken the bonding between S and the Au substrate.

**AUTHOR INFORMATION**
**\*Corresponding author**
Q.Guo@bham.ac.uk, Tel. +44 1214144657

**REFERENCES**

[1] Love, J. C.; Estroff, L. A.; Kriebel, J. K.; Nuzzo, R. G.; Whitesides, G. M. Self-assembled monolayer of thiolates on etals as a form of nanotechnology. *Chem. Rev*. **2005**, *105*, 1103-1169.

[2] Kind, M.; Wöll, Ch. Organic surfaces exposed by self-assembled organothiol monolayers: Preparation, characterization, and application. *Prog. Surf. Sci*. **2009**, *84*, 230-278.

[3] Maksymovych, P.; Voznyy, O.; Dougherty, D. B.; Sorescu, D. V.; Yates, J. T., Jr. Gold adatoms as key structural component in self-assembled monolayers of organosulfur molecules on Au(111). *Prog. Surf. Sci*. **2010**, *85*, 206-240.

[4] Schreiber, F. Structure and growth of self-assembled monolayers. *Prog. Surf. Sci*. **2000**, *65*, 151-256.

[5] Vericat, C.; Vela, M. E.; Benitez, G.; Carro, P.; Salvarezza, R. C. Self-assembled monolayers of thiols and dithiols on gold: new challenges for a well-known system. *Chem. Soc. Rev*. **2010**, *39*, 1805-1834.

[6] Guo, Q.; Li, F. S. Self-assembled alkanethiol monolayers on gold surfaces: resolving the complex structure at the interface by STM. *Phys. Chem. Chem. Phys*. **2014**, *16*, 19074-19090.

[7] Jadzinsky, P.D.; Calero, G.; Ackerson, C.J.; Bushnell, D. A.; Kornberg, R. D. Structure of a thiol monolayer-protected gold nanoparticle at 1.1 angstrom resolution. *Science* **2007**, 318, 430-433.

[8] Negishi, Y. *et al*. A critical size for emergence of nonbulk electronic and geometric structures in dodecanethiolate-protected Au clusters. *J. Am. Chem. Soc*. **2014**, 137, 1206-1212.

[9] Dass, A.; Theivendran, S.; Nimmala, P. R.; Kumara, C.; Jupally, V. R.; Fortunelli, A.; Barcaro, G.; Zuo, X.; Noll, B. C. $Au_{133}(SPh-tBy)_{52}$ nanomolecules: x-ray crystallography, optical, electrochemical, and theoretical analysis. *J. Am. Chem. Soc. **2015**, 137,* 4610-4613.

[10] Jensen, K. M. O.; Juhas, P.; Tofanelli, M. A.; Heinecke, C. L.; Vauhgan, G.; Ackerson, C. J.; Billinge, S. J. L. Polymorphism in magic-sized $Au_{144}SR_{60}$ clusters. *Nat. Commun*. **2016**, 6, 11859. DOI: 10.1038/ncomms11859.

[11] Zeng, C.; Liu, C.; Chen, Y.; Rosi, N. Jin, R. Atomic structure of self-assembled monolayer of thiolate on a tetragonal $Au_{92}$ nanocrystal. *J. Am. Chem. Soc*. **2016**, 138, 8710-8713.

[12] Hakkinen, H. The gold-sulfur interface at the nanoscale. *Nat. Chem*. **2012**, *4*, 443-455.

[13] Tang, L.; Li, F. S.; Guo, Q. Complete structural phases for self-assembled methylthiolate monolayers on Au(111) *J. Phys. Chem. C*. **2013**, *117* (41), 21234-21244.

[14] Gao, J-Z.; Lin, H-P.; Qin, X.; Zhang, X.; Ding, H-X.; Wang, Y. T.; Rokni Fard, M.; Kaya, D.; Zhu, G.; Li, Q.; Pan, M.; Guo, Q. Probing phase evolutions of Au-methyl-propyl-thiolate self-assembled monolayers on Au(111) at molecular level. *J. Phys. Chem. B*. **2018**, *122*, 6666-6672.

[15] Gao, J-Z.; Li, F. S.; Guo, Q. Mixed methyl- and propyl-thiolate monolayers on the Au(111) surface. *Langmuir* **2013**, *29*,11082-11086.

[16] Jiang, De-en; Dai, S. Diffusion of the linear CH3S-Au-SCH3 complex on Au(111) from first principle. *J. Phys. Chem. C*. **2009**, *113*, 3763-3766.

[17] Yu, M.; Bovet, N.; Satterley C. J. *et al*. True nature of an archetypal self-assembled system: Mobile Au-thiolate species on Au(111). *Phys. Rev. Lett*. **2006**, *97*, 166102.

[18] Gao, J-Z.; Li, F. S.; and Guo, Q. Balance of forces in self-assembled monolayers. *J. Phys. Chem. C* **2013**, *117*, 24985-24990.

[19] Li, F. S., Tang, L.; Voznyy, O.; Gao, J-Z., and Guo, Q. The striped phases of ethylthiolate monolayers on the Au(111) surface: a scanning tunneling microscopy study. *J. Chem. Phys*. **2013**, *138*, 194707.

[20] Gao, J-Z.; Li, F.S.; Zhu, G.; Yang, Z.; Lu, H.; Lin, H-P.; Li, Y.; Pan, M-H.; Guo, Q. Spontaneous breaking and re-making of the RS-Au-SR staple in self-assembled ethylthiolate/Au(111) interface. *J. Phys. Chem. C*. **2018**, *122*, 19473-19480.

[21] Kondoh, H.; Nozoye, H. Low-temperature ordered phase of methylthiolate monolayers on Au(111). *J. Phys. Chem. B* **1999**, *103*, 2585-2588.

[22] Li, F-S.; Tang, L.; Gao, J-Z.; Zhou, W-C.; Guo, Q. Adsorption and electron stimulated dissociation of ethanethiol on Au(111). *Langmuir* **2012**, *28*, 11115-11120.

[23] Maksymovych, P.; Sorescu, D. C.; Voznyy, O.; Yates, Jr. J. T. Hybridization of phenylthiolate- and methylthiolate-adatom species at low coverage on the Au(111) surface. *J. Am. Chem. Soc*. **2013**, *135*, 4922-4925.